Surface and Bulk Spin Ordering of Antiferromagnetic Materials: NiO(111)

Antoine Barbier,[1,*] Cristian Mocuta,[2,3] Wolfgang Neubeck,[3] Mattia Mulazzi,[3,4] Flora Yakhou,[3] Karine Chesnel,[5] Albéric Sollier,[3] Christian Vettier,[6] and François de Bergevin[3]

[1]*CEA-Saclay, DSM/DRECAM/SPCSI, 91191 Gif-Sur-Yvette, France*
[2]*Max-Planck-Institut für Metallforschung, Heisenbergstrasse 3, D-70569 Stuttgart, Germany*
[3]*ESRF, 6 Rue Jules Horowitz, BP 220, 38043 Grenoble Cedex 9, France*
[4]*ELETTRA, Area Science Park, S.S.14 Km163.5, 34012 Basovizza(TS), Italy*
[5]*ALS, LBNL, 1 cyclotron road, Berkeley California 94720, USA*
[6]*ILL, 6 Rue Jules Horowitz,BP 156, 38042 Grenoble Cedex 9, France*

(Received 13 February 2004; published 15 December 2004)

We present a study of the prototypical NiO(111) antiferromagnet by nonresonant surface x-ray magnetic scattering. Direct access to the antiferromagnetic surface and bulk spin ordering is demonstrated. Our data support a first order antiferromagnetic to paramagnetic transition. A quantitative determination of the magnetization profile is proposed. It is shown that the NiO(111) surface spins remain ordered at higher temperatures than in the bulk and that the blocking temperature in exchange coupled ferromagnetic-NiO interfaces is most likely related to an *S*-domain structure loss occurring 25 K below the Néel temperature.

DOI: 10.1103/PhysRevLett.93.257208 PACS numbers: 75.70.Rf, 68.47.Gh, 75.50.Ee, 78.70.Ck

Antiferromagnetism had to wait until the pioneering work of Néel [1] to be reasonably understood in bulk materials [2], because of the lack of macroscopic magnetization in such materials and hence the lack of techniques capable of providing information about the spin arrangements in antiferromagnets. The resulting experimental limitations are even more stringent for surface investigations. Recently, interest in spin ordering at antiferromagnetic (AF) interfaces with ferromagnetic (F) layers [3,4], an effect referred to as exchange bias [5–7], has strongly increased by virtue of their implementation in a large panel of technological important fields that rely on magnetic exchange-coupling and spin electronics [8,9]. Exchange bias at a F-AF interface provides an unidirectional magnetic anisotropy and is evidenced by a hysteresis loop shift. The thus obtained magnetic reference state is a key feature in modern magnetic field sensors. The temperature at which the exchange bias vanishes (blocking temperature, T_B) is the one relevant for applications. Although known to be related to—and often different from—the Néel temperature ($T_N = 523.6 \pm 0.2$ K for NiO [10]) at which the AF order vanishes, the understanding of T_B as well as the AF behavior in systems with reduced dimensionality are still a challenging subject of fundamental research [11–13]. The overall knowledge of the spin ordering in AF materials remains limited. For example, even the long standing renormalization group theory [14] first order nature of the Néel transition in rock-salt oxides prediction has not yet received a conclusive experimental confirmation. Within this framework determining the magnetization profile inside antiferromagnets and more generally setting-up techniques enabling the investigation of the AF spin order at surfaces and interfaces as well as the understanding of the associated critical phenomena is especially important and challenging. In order to tackle these open questions we have developed and applied to the prototypical NiO(111) AF surface, which has a well known structure and allows model sensor elaboration [3], the nonresonant surface x-ray magnetic scattering technique [Fig. 1(a)]: a difficult task considering that NiO(111) exhibits an AF spin order parallel to the surface only. Indeed, none of the previously developed techniques [10,15–17] were able to investigate its surface versus bulk AF order because of large charge buildup, low L-edge energy, lack of in-surface-plane AF spin order and systematic charge and magnetic scattering pattern mixing, respectively.

We investigated high quality ($\sim 0.02°$ surface mosaic spreads) single crystalline NiO(111) surfaces [18] kept under vacuum (10^{-6} mbar). The AF order in NiO originates from the superexchange coupling of Ni atoms in alternating (111) planes through oxygen $2p$ electronic orbitals. Ni atoms belonging to the same (111) plane experience a ferromagnetic coupling: their spins are all lying in this plane along the three $[11\bar{2}]$ directions (S domains). The resulting magnetic structure is identical to the structural ordering except a double lattice mesh along the four [111] directions [Fig. 1(b)] (T domains). Our surfaces exhibit the simplest domain structure made of S domains only [19].

In order to disentangle the magnetic and structural contributions we used grazing incidence x-ray magnetic scattering (GIXMS) [Fig. 1(a)] that may very roughly be understood as the combination of x-ray magnetic scattering, based on the interaction between the electron spin and the electromagnetic radiation field [20] and grazing incidence x-ray diffraction (GIXD) that exploits surface refraction effects of the charge scattering close to the critical angle α_c for total external reflection of x rays [21]. At

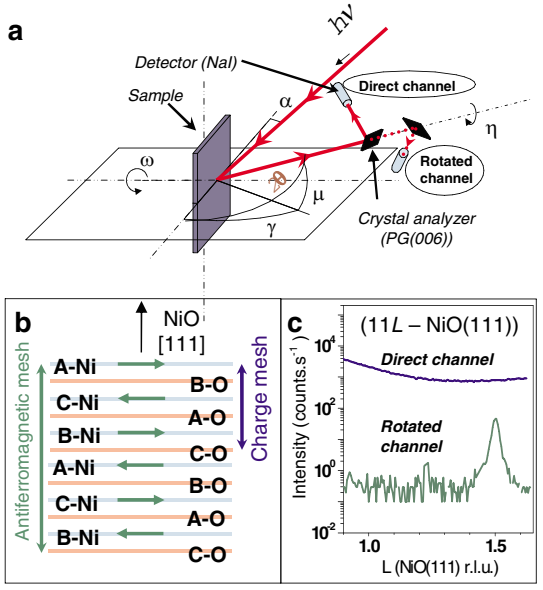

FIG. 1 (color online). Principle of the GIXMS technique. (a) Experimental geometry of the magnetic surface diffraction experiment with a vertical sample surface and a horizontal polarization of the incident x-ray beam. The angles are defined as follows: α is the angle of the incident beam with the surface, ω is the azimuthal sample rotation, 2θ (twice the Bragg angle) is the deviation of the diffracted beam, γ and μ are the in and out-of-plane angles defining the detector position, and η the orientation of the crystal analyzer and detector with respect to the diffracted beam in a plane perpendicular to the diffracted beam. (b) Drawing of the magnetic and structural unit lattices for NiO(111), A, B, and C correspond to the face centered cubic lattice successive plane stacking, horizontal arrows indicate Ni atom spin orientations. (c) Comparison of the signals obtained using both channels during a linear scan along the (11L) reciprocal space direction taken at $\alpha_i = 0.35°$.

variance with the Thompson charge scattering [direct channel with $\tan(\eta) = \tan(\gamma) \times \sin(\mu)$], XMS produces a rotation of the polarization [22] [rotated channel with $\tan(\eta - \frac{\pi}{2}) = \tan(\gamma) \times \sin(\mu)$]. Although GIXMS is not limited to nonresonant conditions, these define the best settings to probe spin ordering; they ensure best polarization analysis, kinematical scattering depending only on AF order, and a direct measure of the magnetization which is then proportional to the square root of the magnetic peak intensity. An incident photon energy of 7981 eV ($\alpha_c = 0.36°$) and a PG(006) crystal analyzer at its Brewster angle with a 99.98% polarization rejection efficiency were used. Following convention, the crystallographic basis vectors for the surface unit cell describe the triangular (111) lattice. They are related to the bulk basis by $\mathbf{a}_{\text{surf}} = [\bar{1}10]_{\text{bulk}}/2$, $\mathbf{b}_{\text{surf}} = [0\bar{1}1]_{\text{bulk}}/2$, and $\mathbf{c}_{\text{surf}} = [111]_{\text{bulk}}$. The L index describes the perpendicular momentum transfer (in reciprocal lattice units). AF reflections are expected at half-distance between successive charge Bragg peaks along L. Figure 1(c) reproduces a room temperature reciprocal space scan along the $(11L)$ direction in the direct and rotated channels. It shows the signals corresponding to the $(11L)$ surface charge scattering and to the magnetic $(11\frac{3}{2})$ diffraction peak that amounts 1% of the minimum of the surface scattering in agreement with the calculated cross sections [21,22].

The magnetic peak intensity and shape were investigated with respect to α_i for all accessible reflections [Fig. 2–$(11\frac{3}{2})$ reflection]. Down to $\alpha_i \sim 3°$ the signal remains roughly equivalent to the one obtained for a symmetric diffraction geometry (top plot in Fig. 2, inset). Further decreasing α_i leads to a peak broadening perpendicularly to the surface and smaller intensities due to the decreasing thickness of material participating in the scattering. The scattered intensity was determined through additional quantitative rocking scans performed at the peak maximum. The intensity evolution of the magnetic peaks with respect to α_i (Fig. 2) matched almost perfectly the typical surface refraction effects. The penetration depth [21] at $\alpha_i = 0.3°$ (respectively, $\alpha_i = 3°$) is 3.5 nm (respectively, 2 μm) allowing one to investigate surface critical phenomena [23] versus bulklike behaviors. Importantly, GIXMS is sensitive to the in-surface-plane S-domain distribution through the deviation from the P3 space group: peaks of same momentum transfer and equivalent in GIXD experience an intensity modulation due to the different

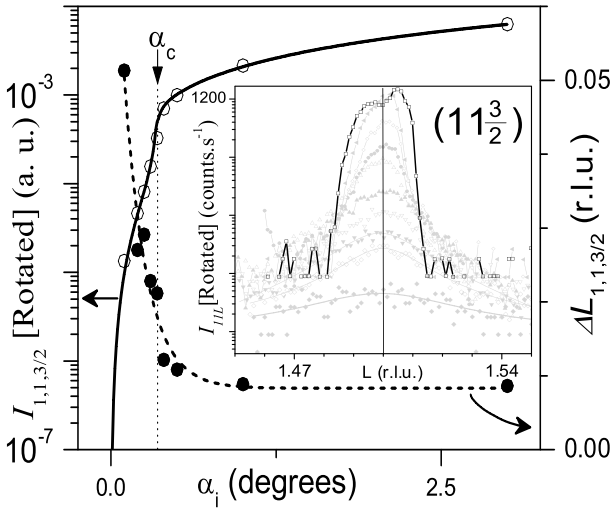

FIG. 2. Refraction effect on AF peaks with respect to α_i at $T = 300$ K. (inset) L scans across the $(11\frac{3}{2})$ NiO AF Bragg peak using the rotated channel at fixed α_i (from bottom to top $\alpha_i = 0.1°$, $0.2°$, $0.25°$, $0.3°$, $0.35°$, $0.4°$, $0.5°$, $1°$, and $3°$—gray curves) compared to a scan taken in the symmetric geometry ($\alpha_i \sim 9.45°$—black curve). For the smallest angles fitted Lorentzian lines are included. (main panel) (Left ordinate) Integrated intensity of the $(11\frac{3}{2})$ peak after active surface area correction (○) and the best fit (solid line) surface refraction law; magnetic and charge scattering exhibit identical α_c. (Right ordinate) $(11\frac{3}{2})$ peak L widths (●) and an exponential decay law (dashed line) included as a guide for the eye.

S-domain populations [19]. This is a genuine feature of GIXMS although for a quantitative investigation of the mean AF order a complete magnetic peak family (same momentum transfer) must be measured.

Complete peak families were considered to explore the Néel transition of NiO(111) in surface and bulk sensitive conditions (Fig. 3). All measurements were made after temperature stability within 0.2 K was reached without any surface lattice parameter evolution [24]. The deduced magnetization [22], M, was determined within 2.5% and is the AF to paramagnetic (P) transition order parameter. Surprisingly, above a special temperature $T_S(\cong T_N\text{-}25)$, for bulk and surface sensitive conditions, the $P3$ symmetry is restored, the otherwise large intensity differences for a given momentum transfer vanish (lower graphs in Fig. 3 for $\alpha_i = 3°$). These measurements indisputably show that the AF-P transition proceeds within *two steps*: at $T = T_S$ the inequivalent S-domain structure is lost whereas at $T = T_N$ any remaining AF order vanishes. To the best of our knowledge such a two-step Néel transition has not been previously evidenced. The in-depth understanding of the $P3$ symmetry recovering at T_S will require additional studies but could tentatively be explained by high frequency thermal fluctuations within S domains [13], loss of the S-domain structure or identical S-domain populations. More importantly, at $T = T_S$ the in-surface-plane magnetic anisotropy, which is mandatory for the onset of exchange bias, is lost and hence $T = T_S$ must be understood as the highest temperature at which exchange coupling of NiO with an adjacent ferromagnetic layer is possible, which is by definition the highest possible blocking temperature. Our present report evidences the direct link between the empirical known blocking temperature and the Néel transition.

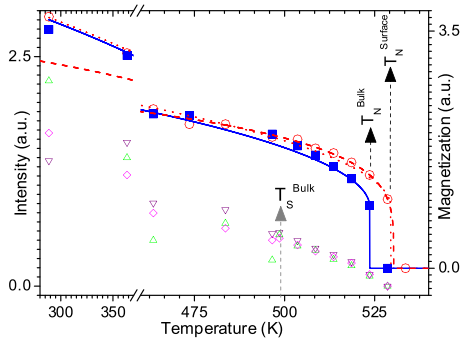

FIG. 3 (color online). Magnetic intensity and magnetization with respect to T. The magnetic intensities were obtained through rocking scans corrected for the L width, surface active area, electrical field strength, incident beam intensity, and corresponding charge scattering (constant internal normalization). (Left ordinate) Bulk sensitive ($\alpha_i = 3°$) diffracted intensities of the $(\bar{1}\,\bar{1}\,\frac{3}{2})$ (∇), $(1\bar{2}\,\frac{3}{2})$ ($\triangle$), and $(2\bar{1}\,\frac{3}{2})$ ($\diamond$) AF Bragg peaks with respect to temperature. The individual peak intensity modulation is related to the in-surface-plane AF S domain structure and vanishes at T_S. The overall evolution for $\alpha_i = 0.3°$ is very similar and the individual intensities collapse again $\sim$25 K before the surface Néel transition temperature is reached. (Right ordinate) Experimental surface ($\alpha_i = 0.3°$, $\bigcirc$) and bulk ($\alpha_i = 3°$, $\blacksquare$) magnetizations derived from the $(11\frac{3}{2})$ peak family. Calculated magnetizations for first order Néel transition ($\kappa = 31.6$, $\epsilon = 100$, $\zeta = 0.1$, $T_N - T_0 = 25$ K) for bulk (solid line, $T_N = 523.6$ K) and surface (dotted line, $T_N = 529.5$ K), and calculated magnetization for a second order surface transition (dashed line, $T_N = 530.3$ K, $\beta = 0.22$). Abscissa axis breaks enlarge the important Néel transition temperature range.

The surface and bulk magnetizations start diverging fairly above 500 K only, thus the thermal gradient in the sample was negligible. Considering a second order description for the phase transition leads to a bulk critical exponent $\beta_b \sim 0.25$. Close to T_N, β_b reaches 0.30 ± 0.02 which is compatible with the $3d$-Ising model, the class of bulk critical phenomena showing the smallest $(5/16)$ β value [25]. To the contrary, the surface critical exponent $\beta_s = 0.22 \pm 0.02$ remains by far above the value $(\frac{1}{8})$ for the corresponding $2d$-Ising model. Measurements made at $\alpha_i = 0.2°$ and $\alpha_i = 0.3°$ were found, after normalization, to superimpose perfectly at each T ruling out an eventual thin film effect. A description in terms of second order phase transition appeared to be unsatisfactory in the context of existing models. Within a first order description of a discontinuous transition, $M \propto (|\kappa| + \sqrt{[|\kappa|^2 - 4\epsilon\zeta(T - T_0)]})/(2\epsilon)$ with $\zeta(T\text{-}T_0)$, κ, and ϵ the coefficients of the development of Landau's free energy and T_0 the temperature for which the P phase starts to be metastable inside the stable AF phase. The fitting procedure shows that with $T_S \cong T_0$ the magnetization is very well reproduced (Fig. 3) for bulk and surface with Néel temperatures of 523.6 ± 0.9 K and 529.5 ± 0.9 K, respectively. Our findings support thus rather a discontinuous AF-P transition for NiO, which is a long standing theoretical renormalization group theory prediction [14], although the transition is very smooth because of a large T_N-T_0 value. An examination of the individual scans shows constant peak widths upon approaching the Néel transition, because of the limited x-ray penetration depth at $\alpha_i = 0.3°$ the characteristic magnetic length must thus extend at least to 10 nm. Since neutron scattering experiments situate this length below 20 nm [26], a value of $D = 15 \pm 5$ nm is a good approximation for the magnetic correlation length. From the bulk *versus* surface ω widths we obtain the lateral domain size $\xi = 163$ nm that is the maximal extend of a given domain. The domain size does not limit the magnetic correlation size in our samples. Importantly, and whatever the order of the transition, the surface T_N is larger than the bulk one by $\Delta T_N = 5.9 \pm 1.8$ K, a value similar to a previous finding on NiO(001), a surface exhibiting a specific 2D AF spin ordering, by metastable helium atom diffusion, a technique sensitive to the top surface layer AF order only [10], confirming the high surface sensitivity of our GIXMS approach. This may also indicate that ΔT_N

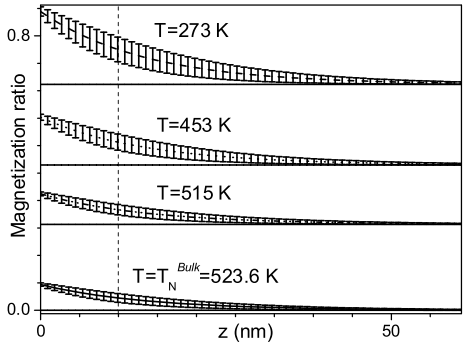

FIG. 4. Magnetization profiles in NiO(111) with respect to z and T for $D = 15 \pm 5$ and $\Delta = 0.32 \pm 0.02$. For each T the asymptotic horizontal line is the bulk magnetization.

may be an intrinsic thermodynamical property of NiO rather than linked to a particular surface orientation or 2D ordering process [which is not relevant for NiO(111)]. The larger surface T_N necessarily stands for an enhanced surface coupling, J_s, with respect to the bulk coupling, J, with $J_s = J(1 + \Delta)$. From our experimental ΔT_N value we find $\Delta = 0.32 \pm 0.02$ [27]. The knowledge (Fig. 3) of the bulk (respectively, surface) magnetization $M_b(T)$ [respectively, $M_s(T)$] fully determines the magnetization profile (Fig. 4) $M(T, z) = M_b(T) + \Delta \times M_s(T) \times \exp(\frac{-z}{D})$, where z is the depth inside the sample from the top surface layer. The depth extension of the perturbation induced by the surface specific contribution to the total magnetization increases for decreasing temperatures leading to the idea that the AF order sets in from the surface toward the bulk and extends deeply into the crystal. The clarification of the eventual role of the higher surface T_N and of unequal S domain populations in the setting up of the unidirectional magnetic exchange coupling with an adjacent magnetically saturated ferromagnetic layer when annealing is performed above T_N will require further work.

The present results provide key features to understand the AF order at NiO(111) surfaces as well as some aspects of unidirectional magnetic exchange anisotropy and illustrate the usefulness of the GIXMS technique. It is a genuine surface *versus* bulk technique that gives simultaneous access to magnetic and structural order, that may be rendered element specific *via* resonant scattering conditions, that enables the nondestructive study of buried interfaces, that allows separating the magnetism of individual domains (like S and T domains for NiO) and is not limited by the absence of specific in-surface-plane spin ordering.

We acknowledge gratefully the ID-20 and ID-16 beam line staffs for efficient help, development and financial and technical support, in particular, G. Pepellin for software developments, P. Bernard and J.-P. Valade for technical assistance and development as well as M. Gautier-Soyer for critical reading of the manuscript.

*Electronic address: abarbier@cea.fr

[1] L. Néel, J. Phys. Radium **15**, 225 (1954).
[2] B. D. Cullity, *Introduction to Magnetic Materials* (Addison-Wesley Publishing Company, Philippines, 1972).
[3] C. Mocuta *et al.*, Phys. Rev. B **68**, 14 416 (2003).
[4] H. Ohldag *et al.*, Phys. Rev. Lett. **86**, 2878 (2001).
[5] W. H. Meiklejohn and C. P. Bean, Phys. Rev. **102**, 1413 (1956).
[6] J. Nogués and I. Schuller, J. Magn. Magn. Mater. **192**, 203 (1999).
[7] R. L. Stamps, J. Phys. D **33**, R247 (2000).
[8] I. Žutić, J. Fabian, and S. D. Sarma, Rev. Mod. Phys. **76**, 323 (2004).
[9] S. S. P. Parkin *et al.*, J. Appl. Phys. **85**, 5828 (1999).
[10] M. Marynowski, *et al.*, Phys. Rev. B **60**, 6053 (1999).
[11] P. J. van der Zaag *et al.*, Phys. Rev. Lett. **84**, 6102 (2000).
[12] O. de Haas *et al.*, Phys. Rev. B **67**, 054405 (2003).
[13] S. Mørup and C. Frandsen, Phys. Rev. Lett. **92**, 217201 (2004).
[14] D. Mukamel and S. Kinsky, Phys. Rev. B **13**, 5078 (1976).
[15] A. Scholl *et al.*, Science **287**, 1014 (2000).
[16] N. Bernhoeft *et al.*, J. Magn. Magn. Mater. **140–144**, 1421 (1995).
[17] G. M. Watson *et al.*, Phys. Rev. Lett. **77**, 751 (1996).
[18] A. Barbier, C. Mocuta, and G. Renaud, Phys. Rev. B **62**, 16056 (2000).
[19] W. Neubeck *et al.*, Phys. Rev. B **63**, 134430 (2001).
[20] F. D. Bergevin and M. Brunel, Acta Crystallogr. Sect. A **37**, 314 (1981).
[21] R. Feidenhans'l, Surf. Sci. Rep. **10**, 105 (1989).
[22] S. W. Lovesey and S. P. Collins, *X-Ray Scattering and Absorption by Magnetic Materials* (Clarendon Press, Oxford, 1996).
[23] H. Dosch, *Critical Phenomena at Surfaces and Interfaces* (Springer-Verlag, Berlin, 1992).
[24] All measurements were made on beam line ID-20 at the European Synchrotron Radiation Facility (Grenoble, France) which delivers an undulator beam with less than 0.1% incident vertical polarization. Thermal stability was typically reached ~4 h after changing the temperature set point.
[25] K. Binder and P. C. Hohenberg, Phys. Rev. B **6**, 3461 (1972).
[26] W. L. Roth, Phys. Rev. **111**, 772 (1958).
[27] K. Binder and P. C. Hohenberg, Phys. Rev. B **9**, 2194 (1974).